Journal of Crystal Growth 318 (2011) 733–736

Contents lists available at ScienceDirect

Journal of Crystal Growth

journal homepage: www.elsevier.com/locate/jcrysgro

Growth and spectroscopic characteristics of Er-doped CeF_3 crystal

Qingguo Wang [a,b], Liangbi Su [a], Hongjun Li [a], Lihe Zheng [a], Huili Tang [a,b], Xin Guo [a,b], Jun Xu [a,*]

[a] Key Laboratory of Transparent and Opto-Functional Advanced Inorganic Materials, Shanghai Institute of Ceramics, Chinese Academy of Sciences, Shanghai 201800, People's Republic of China
[b] Graduate School of the Chinese Academy of Science, Beijing 100039, People's Republic of China

ARTICLE INFO

Available online 23 October 2010

Keywords:
A1. Up-conversion
A1. Luminescence spectra
A2. TGT Method
B1. Yb,Er-doped CeF_3

ABSTRACT

Er-doped and Yb,Er-doped CeF_3 single crystals were grown by Temperature Gradient Technique (TGT) method. The UV–VIR–NIR absorption spectra, near-infrared emission spectra, and $^4I_{13/2}$ decay curves were measured. The infrared to visible up-conversion emission of Er^{3+} wasn't observed in Yb,Er-doped CeF_3 crystal. The efficiency of nonradiative energy transfer from Yb^{3+}($^2F_{5/2}$ level) to Er^{3+}($^4I_{11/2}$ level) was 43.3%. The measured luminescence lifetimes of the ~1.5 μm emission for CeF_3:Yb,Er crystal was 1.91 ms, with quantum efficiency up to 62%.

1. Introduction

Infrared-emitting rare-earth doped materials have been extensively used in fiber amplifiers, solid-state lasers, telecommunications, optoelectronics and remote sensing applications [1]. Laser emitting in the 1.5–1.6 μm spectral range are known since 1962, when Kiss and Duncan have obtained oscillations in an Er-doped $CaWO_4$ crystal [2]. Because of the broad emission at the eye-safe wavelength of 1.5 μm, occurring between the first excited level $^4I_{13/2}$ and the ground level $^4I_{15/2}$ of Er^{3+} ions, Er^{3+} doped laser materials have attracted much more interest. Soon the first pulsed operation of the Er,Yb:glass laser was reported [3]. Yb^{3+} is usually added as the sensitizer to increase the pump absorption efficiency, due to the resonant energy transfer from Yb^{3+}($^2F_{5/2}$) to Er^{3+}($^4I_{11/2}$) at an energy ~10,000 cm^{-1} [4].

With the development at the end of 1980s of new InGaAs laser diodes emitting at 980 nm [5] the realization of a CW erbium laser became possible and the requirements for erbium glass have been modified. CW diode-pumped operation of Er:glass laser is limited at several hundred milliwatts of output power mainly due to thermal defects inside the active element intensified by the low thermal conductivity of the glass host [6]. Because of the high thermal conductivity, a number of erbium-doped crystals were investigated in the search for the best active medium for a CW diode-pumped 1.5 μm laser, but typical slope efficiencies were below 10% [7,8] (the typical slope efficiency of Yb, Er:glass laser is about 20–30% [9]). The main reason is the low branching ratio of ~0.1–0.2 for the 1.5 μm emission. According to the references, one of the methods to improve this branching ratio is co-doping with Ce^{3+} as the deactivator. Due to the phonon-assisted energy transfer between Er^{3+} and Ce^{3+} which facilitates the population of the $^4I_{13/2}$ level and simultaneously decreases up-conversion losses, the branching ratio improves from ~0.1–0.2 to ~0.8–0.9 [10]. In another work, the branching ratio of $^4I_{11/2} \rightarrow {}^4I_{13/2}$ transition of Er^{3+} in Er/Yb/Na/Ce:CaF_2 crystal was improved about 40 times by the deactivating effect of Ce^{3+} [11]. But they also found that when crystals grown with several kinds of impurities, the quality and the thermal properties of the crystals became worse. Then, some host materials which contain Ce^{3+} ions were studied. For example, Yb/Er:CeF_3 nanoparticles were synthesized by hydrothermal process, and its internal quantum efficiency of 1.5 μm emission reached up to 75% and without visible up-conversion luminescence [13].

In this work, CeF_3 single crystals doping of Er^{3+} and Yb^{3+} were grown by a temperature gradient technique (TGT). Then we will discuss the spectroscopic properties of the crystals.

2. Crystal growth

The equipment of TGT for crystal growth of rare-earth-doped CeF_3 single crystals is as described in Ref. [12]. The raw materials with their purities in parentheses were CeF_3(99.99%), ErF_3(99.99%), YbF_3(99.99%) and PbF_2(99.99%). Three kinds of starting powder were prepared, and the ratio of raw materials were as follows: the first one contained 1.5 at% ErF_3, 7.5 at% YbF_3 and 1 at% PbF_2 mixed in CeF_3 powder (labeled YEC), the second one contained 1.5 at% ErF_3, 1 at% PbF_2 mixed in CeF_3 powder (labeled EC), and the third one contained 7.5 at% YbF_3, 1 at% PbF_2 mixed in CeF_3 powder (labeled YC). The PbF_2 powder was used as an oxygen scavenger. we observed that the emission intensity of 1.5 μm increases with the increase of concentration of YbF_3. The crystals were melted at 1460 °C, and then grown on the seeds with reducing the temperature.

* Corresponding author. Tel.: +86 21 69987109; fax: +86 21 69987109.
E-mail address: xujun@mail.shcnc.ac.cn (J. Xu).

0022-0248/$ - see front matter © 2011 Published by Elsevier B.V.
doi:10.1016/j.jcrysgro.2010.09.085

The concentration of dopant ions in the three crystals were measured by ICP-AES analysis. Optical absorption spectra were recorded by Jasco V-570 UV/VIS/NIR spectrophotometer. The luminescence spectra at 1000–1700 nm were recorded with Triax550 spectrofluorimeter under 980 nm LD pumping. The emission lifetimes for $^4I_{13/2}$ level and $^4I_{11/2}$ level of Er^{3+} and $^2F_{5/2}$ level of Yb^{3+} were measured using a modulated 980, 940 and 808 nm LD with a Tektronix TDS3052 digital oscilloscope to store the temporal decay curves of the fluorescence signals at 1530, 1060 and 1030 nm, respectively. All these measurements were taken at room temperature.

3. Result and discussion

The color of YEC and YC crystals with Yb^{3+} ions are deep yellow, and the color of EC crystal is buff. The X-ray diffraction (XRD) patterns of the YEC sample (Fig. 1) was recorded by the D/max 2550 V X-ray diffraction analysis (X-ray generator: power 18 kW (40 kV, 450 mA), stability −0.01%; Goniometer accuracy: 0.002°(2θ)). We identified the pattern with the standard cards, and found that it was well consistent with the ICSD#: 081674 card.

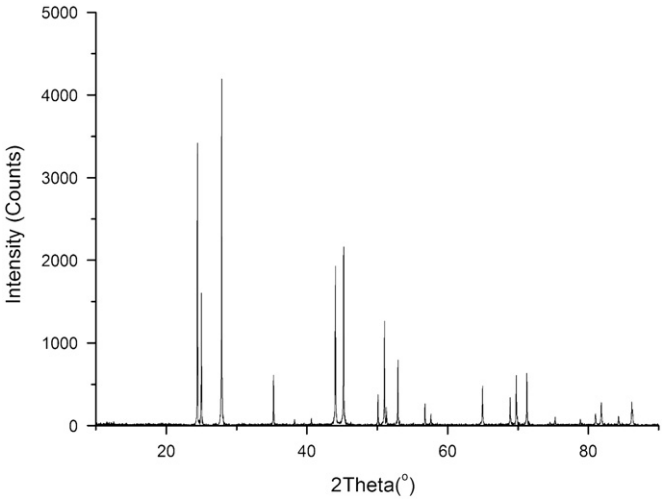

Fig. 1. The XRD pattern of YEC crystal.

The samples for ICP-AES analysis were selected in the crystals with different distance from the seed. Fig. 2 shows the concentrations of the dopant ions at different locations of the crystals. The abscissa shows the distances of the locations of the samples from the seed. Then, we calculated the effective segregation coefficient with the formula [14,15]: $k_{eff}=C_S/C_L$, which is the ratio of the concentration of solute in the solid C_S to that in the liquid C_L. At the beginning of crystal growth, C_S is the solute concentration near the seed, and C_L can be replaced with the original concentration of the solute (C_0) approximately. The original concentrations of Yb^{3+} and Er^{3+} are 5.9 and 1.14 wt% for YEC crystal, 1.24 wt% for EC crystal, and 6.05 wt% for YC crystal, respectively. So, the effective segregation coefficients of the dopant ions in the grown crystals were as follows: $k_{eff}(Yb^{3+})=0.44$, $k_{eff}(Er^{3+})=0.26$ for YEC crystal, $k_{eff}(Yb^{3+})=0.15$ for YC crystal and $k_{eff}(Er^{3+})=0.33$ for EC crystal. We think that the reason to the low k_{eff} value is due to the biggish diameter difference between the dopant ions and Ce^{3+} in the crystals. The radius of Yb^{3+}, Er^{3+} and Ce^{3+} are 1.00 Å, 1.03 and 1.15 Å, respectively [16]. So, $\Delta r(Yb^{3+}/Ce^{3+})$ is 13%, and $\Delta r(Er^{3+}/Ce^{3+})$ is 10.4%. The dopant ions cannot enter the crystal lattice effectively and they will enrich in the melt in the growth process. It is also the reason of the increase of the impurities' concentration with increasing the distance from the seed.

Fig. 3 shows the transmittance curve of the CeF_3 crystal. There is a broad absorption band in the region of 2000–3000 cm^{-1}. The absorption band should be corresponding to $^2F_{7/2}\rightarrow{}^2F_{5/2}$ transition of Ce^{3+}. Considering that the cutoff phonon energy for CeF_3 was $\sim$320 cm^{-1} and energy difference of $\Delta E\sim3656$ cm^{-1} between the $^4I_{11/2}\rightarrow{}^4I_{13/2}$ transition of Er^{3+} [17,18], the estimated number of phonons emitted is $\sim$2 in the nonradiative decay from $^4I_{11/2}$ level to $^4I_{13/2}$ level by deactivating of Ce^{3+}, assuming that the phonons involved in the energy transfer are of equal energy.

With pumping at 980 nm, the energy transfer routes between Yb^{3+}, Er^{3+} and Ce^{3+} ions are as depicted in Ref. [11]. The $^4I_{11/2}$ level of Er^{3+} ions will be populated mainly through resonant energy transfer from the $^2F_{5/2}$ level of Yb^{3+} ions, i.e. $^2F_{5/2}+{}^4I_{15/2}\rightarrow{}^2F_{7/2}+{}^4I_{11/2}$. The upper $^4I_{13/2}$ level of Er^{3+} for 1.5 μm emission is populated through the relaxation from the $^4I_{11/2}$ level. In the CeF_3 crystal, the process of phonon-assisted transition $^4I_{11/2}\rightarrow{}^4I_{13/2}$ is dominated by fast phonon-assisted resonant energy transfer between Er^{3+} and Ce^{3+}, i.e. $^4I_{11/2}+{}^2F_{7/2}\rightarrow{}^4I_{13/2}+{}^2F_{5/2}$. We calculated the absorption cross sections of Yb^{3+} and Er^{3+} at 980 nm, and they were 0.904×10^{-20} and 0.14×10^{-20} cm^2, respectively. In other words, the pump-energy absorption efficiency of Er^{3+} in YEC crystal is about 6 times higher than that in EC crystal. And, the luminescence intensity of 1.5 μm emission of YEC

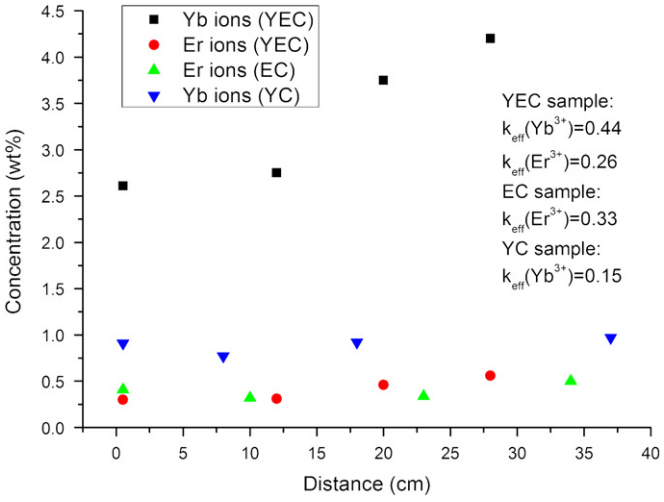

Fig. 2. The concentrations of dopant ions in the three crystals.

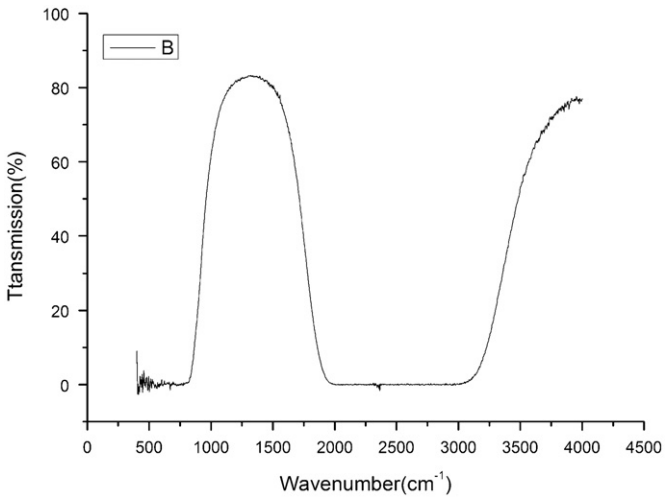

Fig. 3. The transmittance curve of YEC crystal in infrared region.

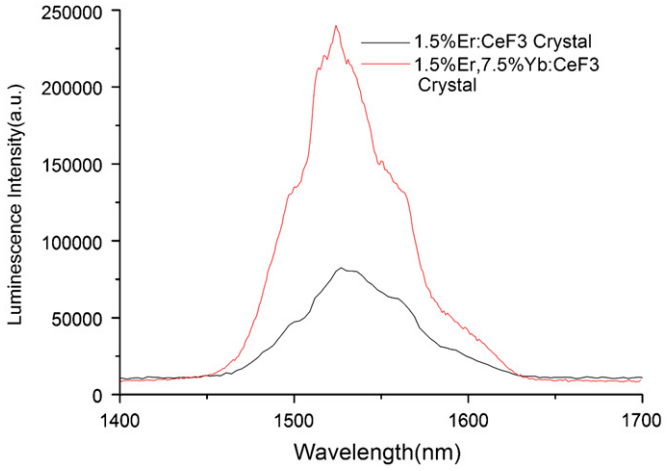

Fig. 4. The luminescence spectra of YEC and EC crystal at 1.5 μm region.

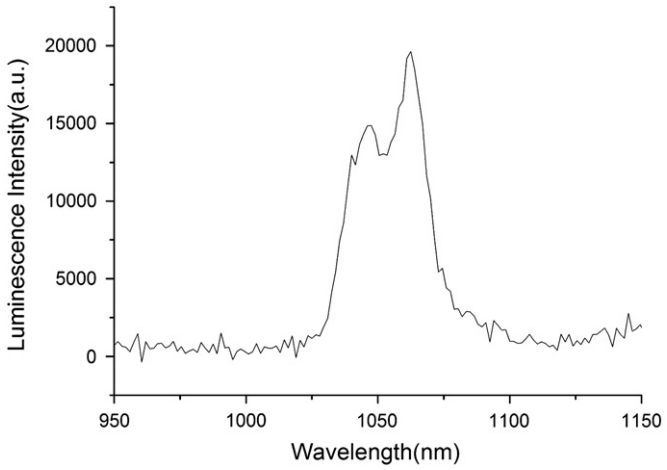

Fig. 5. The luminescence spectra of Er^{3+} ions from the transition $^4I_{11/2} \rightarrow {}^4I_{15/2}$ in 1.5%Er^{3+}:CeF_3 crystal with 808 nm pumping.

sample is about 3 times than that in EC sample (Fig. 4). The fluorescence lifetime of the $^4I_{13/2}$ level of Er^{3+} ions was also measured in this work. The values of $\tau_{EM}(^4I_{13/2})$ are 1.91 and 1.65 ms for YEC and EC crystal, respectively. The radiative lifetime of the $^4I_{13/2}$ level of Er^{3+} ions in CeF_3 crystal was also calculated by Judd–Ofelt Theory [20,21], and its value ($\tau_R(^4I_{13/2})$) was 3.07 ms. So, the quantum efficiency (η) of 1.5 μm luminescence is about 62% according the formula, i.e. $\eta = \tau_{EM}(^4I_{13/2})/\tau_R(^4I_{13/2})$. Then we calculated the emission cross section of 1530 nm emission of YEC and EC samples with F-L equation [19], and they were 1.26×10^{-20} and 1.25×10^{-20} cm^2, respectively.

The excited state absorption and up-conversion luminescence could affect the efficiency of 1.5 μm emission greatly. The luminescence spectra in visible region (~300–800 nm) of the grown YEC crystal was investigated, and it was found that there was no any fluorescence signal in this region. The efficient deactivating effect of Ce^{3+} ions was demonstrated to eliminate the up-conversion of Er^{3+} ions in YEC crystal.

Fig. 5 shows the luminescence spectra of Er^{3+} ions from the transition $^4I_{11/2} \rightarrow {}^4I_{15/2}$ in EC crystal with 808 nm pumping. In YEC crystal, it overlaps with the luminescence spectra of Yb^{3+} ions. The measured fluorescence lifetime of the $^4I_{11/2}$ level ($\tau_{EM}(^4I_{11/2})$) of Er^{3+} ions in EC crystal is about 432 μs. Another important parameter of Er^{3+}/Yb^{3+} co-doped materials is the energy transfer efficiency from Yb^{3+} ions to Er^{3+} ions ($\eta_{Yb \rightarrow Er}$). Its value can be calculated from the following formula, i.e. $\eta_{Yb \rightarrow Er} = 1 - \tau_{Yb,Er}/\tau_{Yb}$. Where τ_{Yb} is the lifetime of the Yb^{3+} $^2F_{5/2}$ level in Yb-single-doped crystal (YC crystal), and $\tau_{Yb,Er}$ is its lifetime in Yb,Er-codoped crystal (YEC crystal) [22]. In our work, it was found that the lifetime of Yb^{3+} ions shortens from 492 μs in YC crystal to 279 μs in YEC crystal. So, the value of $\eta_{Yb \rightarrow Er}$ is about 43.3%. In our opinion, the lifetime reduction is consequence of nonradiative resonant energy transfer from the Yb^{3+} to the Er^{3+} ions.

4. Conclusions

In conclusion, a doping scheme of Er^{3+} and Yb^{3+} in CeF_3 single crystals were grown by TGT method. Broad band luminescence at 1.5 μm was observed under 980 and 940 nm LD pumping. The deactivating effect of Ce^{3+} on the Er^{3+} ions was demonstrated by the increase the integrated emission intensity at 1.5 μm and the elimination of the up-conversion luminescence in visible region under 980 nm pumping. The resonant energy transfer efficiency from Yb^{3+} to Er^{3+} ions was about 43.3%, and the fluorescence quantum efficiency of 1.5 μm reached to 62%.

Acknowledgement

The authors are indebted to the National Science Foundation of China (Grant nos. 60938001 and 60908030) and Science and Technology Commission of Shanghai Municipality (Grant no. 09JC1415300).

References

[1] A.J. Kenyon, Recent developments in rare-earth doped materials for optoelectronics, Prog. Quantum Electron. 26 (2002) 225–284.
[2] Z.J. Kiss, R.C. Duncan, Pulsed and continuous optical maser action in CaF_2-Dy^2, Proc. IEEE 50 (1962) 1531.
[3] E. Snitzer, R. Woodcock, Yb^{3+}-Er^{3+} glass laser (RM-TEMP 3-level laser-energy transfer from Yb^{3+} to Er^{3+}), Appl. Phys. Lett. 6 (1965) 45.
[4] P. Laporta, S. Taccheo, S. Longhi, O. Svelto, Diode-pumped microchip Er-Yb-glass laser, Opt. Lett. 18 (1993) 1232–1234.
[5] M. Okayasu, S. Takeshita, M. Yamada, O. Kogura, M. Horiguchi, M. Fukuda, A. Kozen, K. Oe, S. Uehara, High-power 0.98 μm GaInAs strained quantum well laser for Er^{3+}-doped fiber amplifier, Electron. Lett. 25 (1989) 1563–1565.
[6] N.A. Tolstik, V.E. Kisel, N.V. Kuleshov, V.V. Maltsev, Er, Yb:$YAl_3(BO_3)_4$-efficient 1.5 μm laser crystal, Appl. Phys. B 97 (2009) 357–362.
[7] B. Simondi-Teisseire, B. Viana, A.M. Lejus, J.M. Benitez, D. Vivien, C. Borel, R. Templier, C. Wyon, Room-temperature CW laser operation at similar to 1.55 μm (eye-safe range) of Yb:Er and Yb:Er:Ce:$Ca_2Al_2SiO_7$ crystal, IEEE J. Quantum Electron. 32 (1996) 2004–2009.
[8] A. Diening, E. Heumann, G. Huber, O. Kuzmin, High-power diode-pumped Yb:Er:LSB laser at 1.56 μm, Cnference on Lasers and Electro-Optics (CLEO), 1998 OSA Technical Digest Series, Vol. 6 (Optical Society of America), pp. 299–300.
[9] P. Laporta, S. Taccheo, S. Longhi, O. Svelto, C. Svelto, Erbium-ytterbium microlasers: optical properties and lasing characteristics, Opt. Mater. 11 (1999) 269–288.
[10] Z. Meng, T. Yoshimura, K. Fukue, M. Higashihata, Y. Nakata, T. Okada, Large improvement in quantum fluorescence yield of Er^{3+}-doped fluorozirconate and fluoroindate glasses by Ce^{3+} co-doping, J. Appl. Phys. 88 (2000) 2187–2190.
[11] J. Xu, L.B. Su, H.J. Li, D. Zhang, L. Wen, H. Lin, G.J. Zhao, High quantum fluorescence yield of Er^{3+} at 1.5 μm in an Yb^{3+},Ce^{3+}-codoped CaF_2 crystal, Opt. Mater. 29 (2007) 932–935.
[12] Y.X. Zhou, Growth of high-quality laser Nd-YAG crystals by temperature-gradient technique (TGT), J. Cryst. Growth 78 (1986) 31–35.
[13] M.C. Tan, G.A. Kumar, R.E. Riman, Near infrared-emitting Er- and Yb-Er-doped CeF_3 nanoparticles with no visible upconversion, Opt. Express 17 (2009) 15904–15910.
[14] J.A. Burton, R.C. Prim, W.P. Slichter, The distribution of solute in crystals growth from the melt, J. Chem. Phys. 21 (1953) 1987–1991.
[15] E.V. Zharikov, Yu.D. Zavartsev, V.V. Laptev, S.A. Samoilova, Impurity distribution within the diffusion in the cluster crystallization model, Cryst. Res. Technol. 24 (1989) 751–759.
[16] Goldschmidt, Handbook on Physics and Chemistry of Rare Earths, Vol.1, North-Holland Publishing Company, 1978.

[17] H. Gerlinger, G. Schaack, Crystal-field states of the Ce^{3+} ion in CeF_3: A demonstration of vibronic interaction in ionic rare-earth compounds, Phys. Rev. B 33 (1986) 7438–7450.
[18] M.J.F. Digonnet, Rare Earth Doped Fiber Lasers and Amplifiers, Marcel Dekker, Inc., 1993.
[19] P. Haumesser, R. Gaume, B. Viana, D. Vivien, Determination of laser parameters of ytterbium-doped oxide crystalline materials, J. Opt. Am. B 19 (2002) 2365–2375.
[20] B.R. Judd, Optical absorption intensities of rare-earth ions, Phys. Rev. 127 (1962) 750–761.
[21] G.S. Ofelt, Intensities of crystal spectra of rare-earth ions, J. Chem. Phys. 37 (1962) 511–520.
[22] V.A. Lebedev, V.F. Pisarenko, N.V. Selina, A.A. Perfilin, M.G. Brik, Spectroscopic and luminescent properties of Yb,Er:$LaSc_3(BO_3)_4$ crystals, Opt. Mater. 14 (2000) 121–126.